34th Annual International Conference of the IEEE EMBS
San Diego, California USA, 28 August - 1 September, 2012

Psoriasis Segmentation through Chromatic Regions and Geometric Active Contours

F. Bogo[1], M. Samory[1], A. Belloni Fortina[2], S. Piaserico[2] and E. Peserico[1]

Abstract— **We present a novel approach to the segmentation of psoriasis lesions in "full body" digital photographs potentially involving dozens or even hundreds of separate lesions. Our algorithm first isolates a set of zones that certainly correspond to lesional plaques based on chromatic information, and then expands these zones to achieve an accurate segmentation of plaques through a Geometric Active Contours method. The variability in segmentation between our algorithm and different human operators appears comparable to the variability between human operators.**

I. Introduction

Psoriasis is a chronic, inflammatory multisystem disease that usually appears on the skin. Psoriasis affects $1-3\%$ of the world's population [5]; while currently no cure is known, various treatments can help control symptoms. The most common clinical variant ($80-90\%$ of all cases) is *psoriasis vulgaris*, characterized by circular-to-oval red skin plaques often with silvery white scales; the extent of affected skin can range from minor localized patches to full body coverage [18].

One of the most important parameters for evaluating the seriousness of a psoriasis case is the percentage of the cutaneous surface affected. Lesion area is the highest weight parameter in the Psoriasis Area and Severity Index (PASI – the current "gold standard" in psoriasis scoring) [3] as well as in most alternative, simplified indices [15].

Manually evaluating lesion area by hand is prohibitively time consuming; furthermore, it is often prone to significant margins of error [14]. Automated evaluation of psoriasis lesion area, performed by a computer operating on digital photographs of the patient, promises instead non-invasive, fast, accurate and highly reproducible assessments of lesion area with minimal intervention by the dermatologist [13]. The crucial step in evaluating lesion area is *segmentation*, i.e. classification of all points in the image as part of the lesion or simply part of the surrounding, healthy skin. Most work in the literature focuses on "single lesion" segmentation. This work introduces a robust approach to the segmentation of psoriasis lesions in "full body" digital photographs potentially involving dozens or even hundreds of separate lesions.

The rest of this work is organized as follows. Section II reviews the most significant approaches to psoriasis segmentation in the literature. Section III describes our approach in detail. Section IV provides an experimental evaluation of our techniques over a set of "full body" images from 20 different patients. Section V summarizes our results and discusses their significance before concluding with the Bibliography.

*This work was supported in part by MIUR under PRIN AlgoDeep and by Univ. Padova under proj. AACSE (psoriasis@dei.unipd.it)

[1]Dip. Ing. Informazione, Univ. Padova.
[2]Dip. Medicina, Univ. Padova.

II. Related work

Several different approaches to psoriasis segmentation have been proposed, each with specific strengths and weaknesses. Most reported research focuses on psoriasis vulgaris, due to its vast prevalence over all other forms.

The greyscale thresholding method applied in [16] is simple and efficient, but suffers from extreme sensitivity to illumination variations. [4] [19] [1] rely on Artificial Neural Network (ANN) classification; the ANN paradigm makes it difficult to incorporate expert insight and feedback and, more importantly, is computationally intensive (requiring a training phase per patient). [9] adapts to psoriasis segmentation the powerful approach of $k-$means clustering, requiring rigorous parameter tuning; the same requirement holds for [20], which is based on Multiple Spectral-Spatial Classification. The approach of [6] uses colour distance metrics to classify pixels; when applied to "full body" photographs, this method is not robust with respect to variability in skin texture, colour and illumination.

In most work, segmentation methods are evaluated on sets of less than half a dozen images; each image usually involves only a single lesion. Performance assessment is in terms of misclassified pixels compared to a "ground truth" manually provided by a human operator.

III. A robust segmentation algorithm

Our algorithm pursues two main goals. First, it aims at segmenting *large regions* of the body, possibly including dozens or even hundreds of different lesions. Second, it aims at segmenting *robustly* different patients, tolerating variability in skin pigmentation and lesion appearance.

As a preliminary step, we evaluate strengths and weaknesses in pursuing these two goals of chromatic-based approaches commonly used in single lesion segmentation (Subsection III-A). A straightforward use of these techniques turns out to be ineffective. Thus, we break the whole segmentation process into two simpler phases, mimicking the approach of a human operator. The first phase analyses the whole image and isolates those areas that *certainly* correspond to psoriasis plaques (Subsection III-B). The second phase individually analyses areas isolated during the first phase and accurately determines lesion borders through a Geometric Active Contours methodology (Subsection III-C).

978-1-4577-1787-1/12/$26.00 ©2012 IEEE

A. Psoriasis segmentation in colour space

Human operators detect a lesion by its *contrast* with surrounding skin (e.g. considering differences in skin colour or texture). Accordingly, pixels should be classified as healthy or lesional on the basis of a specific *distance* over a discriminating feature space. Most work in the literature focuses on colour features; in order to detect a set of discriminating ones, we performed a preliminary experimental study applying Principal Component Analysis (PCA) [8] to a dataset of images projected on four different colour spaces.

Our dataset consisted of 20 digital photographs, each of a different patient affected by psoriasis vulgaris. All patients were caucasian. A sizable fraction of all lesions was scaly. Among these 20 photographs, 8 were of legs, 7 of back torsos and arms, and 5 of front torsos and arms. In 8 photographs the patient appeared partially clothed. In some photographs over 95% of the visible skin was healthy, in some more than 50% was lesional. Every photograph involved multiple distinct lesions, in some cases more than 50. Each photograph was independently segmented by two human operators, using a graphic tablet.

We projected each photograph onto four different colour spaces[10] (RGB, Lab, HSV and YUV). Then, we applied PCA to the resulting representations and observed the following:

- When only a small portion of the skin is lesional, projecting the image onto the main one or two Principal Components "erases" psoriasis pixels (i.e. they are confused with noise); this makes standard PCA unsuitable for classification.
- In all cases, one of the Principal Components (but not always the first or even the second one) discriminates between healthy and lesional skin.
- The discriminating Principal Component seems well aligned with the chrominance component V from YUV colour space and the H component from HSV colour space.

V can be seen as the red purity of a colour. Defined as:

$$V(R,G,B) = \frac{1}{2} + \frac{R}{2} - \frac{G+B}{4} \tag{1}$$

V ranges from 1 (for a deep red) to 0 (for its opposite, a strong cyan).

H corresponds to the *hue* – in some sense the dominant wavelength – of a colour. More precisely, consider a point $\langle R,G,B\rangle$ in the RGB colour space (with $0 \leq R,G,B \leq 1$), and let $M = \max(R,G,B)$ and $m = \min(R,G,B)$. $H(\langle R,G,B\rangle)$, measured on the $[0,1)$ interval, is defined as:

$$H(\langle R,G,B\rangle) = \begin{cases} \frac{G-B}{6(M-m)} \mod 1 & \text{if } R \geq G,B \\ \frac{B-R}{6(M-m)} + \frac{1}{3} & \text{if } G \geq B,R \\ \frac{R-G}{6(M-m)} + \frac{2}{3} & \text{if } B \geq R,G \\ undefined & \text{if } M = m \end{cases} \tag{2}$$

Informally, we can think hue as representing colour on a circumference mapped on the interval $[0,1)$, where greens are close to $1/3$, blues to $2/3$, and reds close to 0 and 1; by convention, $H(x) = 0$ if $M = m$. For simplicity, we introduce a *shifted hue* $H'(x) = ((H(x) + 0.06) \mod 1)$ that essentially maps close to 0 all predominantly red pixels, leaving purplish/pink ones close to 1.

The naive projection of patient images on the 2-D space induced by H' and V does not allow accurate classification of pixels (see Figure 1).

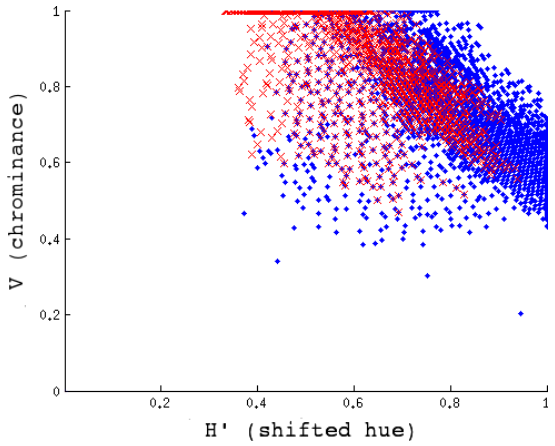

Fig. 1: Projection of a patient photograph on the 2-D space induced by H' (shifted hue) and V (chrominance); healthy pixels (blue squares) are not separable from psoriasis pixels (red crosses).

Separation is hard for two main reasons. First, "full body" images may present distortion and high variability in skin texture, colour and illumination. Second, psoriasis lesions in different body regions of the same patient may be highly inhomogeneous. *Approaches involving thresholding on bimodal colour histograms of skin surface, commonly used for single lesion analysis, cannot provide accurate and robust segmentation in the case of "full body" images.*

B. Chromatic partitioning

While straightforward segmentation of multiple psoriasis lesions in colour space leads to inaccurate results, one can employ chromatic features to solve a related problem: the detection of *at least* one pixel per plaque. This pixel then becomes an *indicator* for the plaque itself.

The first phase of our algorithm analyses "full body" images, isolates patient skin from the background and obtains a set of indicator pixels in the H'-V space. The neighbourhood of each indicator is then expanded through a Geometric Active Contours method during the second phase to accurately determine lesion borders.

Isolation of the skin (healthy or lesional) from the background is an easy task if the digital photograph is taken under appropriate conditions – for example, against a uniform green or blue background. However, in many cases, one has to work with photographs taken in less than ideal conditions, including patients who are partially dressed. We have found that preprocessing based on Region Of Interest (ROI) segmentation similar to that described in [12] is extremely robust and allows isolation of portions of skin with great accuracy.

We then analyse the skin area to extract a set of indicator pixels. For any pixel x, we denote by $\langle H'(x),\ V(x)\rangle$ its colour components in the H'-V colour space. Given an image, a subset S of its pixels is a *complete* set of indicators if at least 90% of the pixels in S are psoriasis pixels and the plaques containing at least one indicator cover more than 90% of the lesional skin. An image contains an *easily separable* complete set if there exist two thresholds $t_{h'}$ and t_v such that the set

$$S = \{x : H'(x) \leq t_{h'}, V(x) \geq t_v\} \tag{3}$$

is a complete set. Analysing our dataset, we were able to extract an easily separable complete set in 85% of the images (see Figure 2).

Fig. 2: Identification of a set of *indicator pixels* (marked in white).

Interestingly, the thresholds varied very little between images. Their average values were $\bar{t}_{h'} = 0.61$ and $\bar{t}_v = 0.93$ (with a standard deviation less than 0.05 for both values). The variety of our dataset suggests these values can be effective in tackling the indicator problem on a wide range of images. While image specific thresholding could lead to more accurate results, Section IV experimentally shows that $\bar{t}_{h'}$ and $\bar{t}_v$ can guarantee good performance with low computational requirements (since one can avoid recomputing different thresholds for each image).

C. Geometric Active Contours

During the second phase, we accurately segment psoriasis lesions in (shifted) hue space through a Geometric Active Contours (GAC) algorithm [11] [17].

Any indicator pixel identified during the first phase can be fed to our GAC algorithm as a "seed" that one can "inflate" to obtain the contour of a lesion. Given an arbitrary indicator pixel, we set as *initial contour* the edges of a 3×3 pixel square centred on the indicator itself. We iteratively evolve this initial contour to maximize a well-determined image-based energy functional (see Figure 3). We found particularly effective the energy functional described in [17].

Formally, a contour $\mathcal{C}$ is the set of zeros of a signed distance function $\phi : \mathbb{R}^2 \rightarrow \mathbb{R}$. ϕ is negative inside the lesion, and positive outside. By modelling the hue of each pixel as a random variable z, we evaluate the probability density functions (pdf) $p_{in}(z,\phi)$ and $p_{out}(z,\phi)$ for the pixels inside and outside $\mathcal{C}$. The *distance* between pixels inside and outside $\mathcal{C}$ is the standard deviation of the difference between the logarithms of $p_{in}(z,\phi)$ and $p_{out}(z,\phi)$. We maximize this distance by maximizing the energy functional:

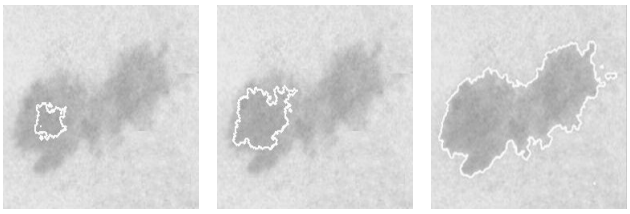

Fig. 3: Progressive adjustment of single lesion segmentation in the GAC framework.

$$E(z,\phi) = \sqrt{\mathcal{E}\left[\left(\log\frac{p_{in}(z,\phi)}{p_{out}(z,\phi)}\right)^2\right] - \mathcal{E}\left[\left(\log\frac{p_{in}(z,\phi)}{p_{out}(z,\phi)}\right)\right]^2} \tag{4}$$

where $\mathcal{E}[f(z)]$ denotes the expected value of $f(z)$. ϕ (and thus $\mathcal{C}$) evolves according to the equation:

$$\frac{\delta\phi}{\delta t} = \bigtriangledown_\phi E(z,\phi) \tag{5}$$

Evolution stops when convergence has been achieved or after a maximum number of iterations.

As mentioned above, the second phase uses indicator pixels as "seeds" for GAC iterations. The "full body" image is projected on the hue space and partitioned into a set of windows of fixed size; windows are small enough to contain, on average, no more than half a dozen plaques. Each window is then analysed iteratively, separately from the others. For each window, we consider the indicator pixel of maximum hue and expand its contour through our GAC algorithm, until the plaque borders are accurately matched. The same procedure is applied again to the indicator pixel of maximum hue among those *not marked* as lesional in the previous step. The process is iterated until all the indicators in the window have been marked as part of a lesion by at least one GAC expansion. If a GAC expansion produces a border intersecting a window margin, then the pixels on the boundary are marked as indicators for the neighbouring window. The phase ends when every indicator has been analysed. If a "seed" for GAC iterations corresponds to a pixel incorrectly marked as lesional in the first phase, then $p_{in}(z,\phi)$ and $p_{out}(z,\phi)$ are highly similar and the initial contour does not evolve.

Figure 4 compares the segmentation produced by our algorithm with that produced by a human operator.

IV. Experimental evaluation

We evaluated our algorithm on the dataset of 20 digital images described in Subsection III-A. During the first phase, we marked as indicators all pixels with shifted hue at most

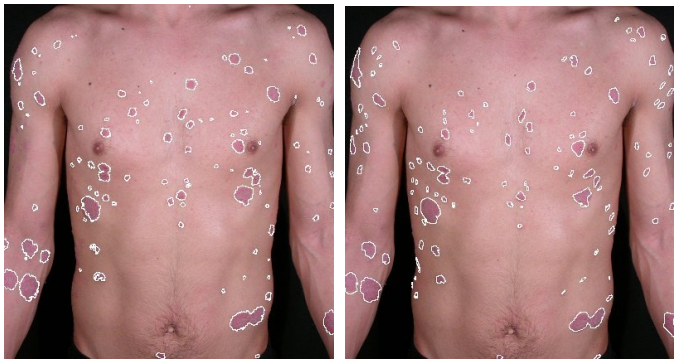

Fig. 4: Segmentation of psoriasis plaques by our algorithm (left) and by a human operator (right).

$\bar{t}_{h'}$ and red purity at least $\bar{t}_v$. During the second phase, each GAC execution was run for at most 400 iterations. For each photograph and each operator, we measured the area of the *misclassified region* – i.e. the number of pixels classified as lesion by the algorithm or by the operator but not by both. This quantity was then, in each photograph, compared to the total lesion area according to the operator.

The area of the misclassified region was 14% of the lesion area according to the first human operator. It was 16% of the lesion area according to the second operator. Misclassification was due mostly to *false negatives* (i.e. psoriasis pixels classified as healthy by our algorithm): scaly lesions containing no dull-red zones were not detected in the first phase. We observed no correlation between misclassification rate and percentage of lesional skin.

In evaluating these results, three things should be kept in mind. First, the photographs were taken in realistic field conditions, with suboptimal illumination, posture etc. Second, and in contrast with most of the literature, our photographs involved a large number of distinct lesions, often at a rather sharp angle with the camera. Third, and perhaps most importantly, it seems fundamentally impossible to achieve considerably better results: we compared the segmentations of the two human operators (as in [2]) and found that the area of the region "misclassified" by the first operator was 9% of the lesion area according to the second. In other words, *the machine-operator variability in assessing the exact lesion borders appears comparable to the variability between different human operators*.

V. Conclusions

Our algorithm combines two steps to accurately detect the borders of psoriasis plaques in "full body" digital photographs involving up to several dozen lesions. The variability in segmentation between our algorithm and different human operators appears comparable to the variability between human operators. Although this does not rule out that other algorithms could outperform ours, any such performance increase would require a methodology different from the "standard" comparison to a human operator to be quantified.

This work is only the first step toward a semi-automated evaluation of the percentage of cutaneous surface affected by psoriasis – and of other characteristics of psoriasis such as erythema or desquamation. To compute the area affected, at the very minimum it should be combined with a model of the 3D curvature of the body. It should also be extended to deal with different skin colours and rarer types of psoriasis (e.g. guttate, inverse, pustular and erythrodermic psoriasis), possibly considering texture features in addition to colour ones. Finally, it would be extremely important to evaluate the variability of the algorithm in assessing the same set of lesions under slightly different postures, zooms and illumination conditions.

References

[1] N.K.A. Abbadi, N.S. Dahir, M.A.A. Dhalimi, and H. Restom. Psoriasis detection using skin color and texture features. *Journal of Computer Science*, 6(6):648–652, 2010.

[2] A. Belloni Fortina, E. Peserico, A. Silletti, and E. Zattra. Where's the naevus? Inter-operator variability in the localization of melanocytic lesion border. *Skin Research and Technology*, 2011.

[3] T. Fredriksson and U. Pettersson. Severe psoriasis–oral therapy with a new retinoid. *Dermatologica*, 157(4):238–244, 1978.

[4] H. Hashim, R. Jarmin, and R. Jailani. Plaque psoriasis diagnosis model with dominant pixel gradation from primary color space. In *Proc. Asian Conference on Sensors and the International Conference on new Techniques in Pharmaceutical and Biomedical Research 2005*, pages 81–86.

[5] C. Huerta, E. Rivero, and L.A.G. Rodriguez. Incidence and risk factors for psoriasis in the general population. *Archives of Dermatology*, 143(12):1559, 2007.

[6] D. Ihtatho, M.H. Ahmad Fadzil, A. Mohd Affandi, and S.H. Hussein. Automatic PASI area scoring. In *Proc. ICIAS 2007*, pages 819–822.

[7] R. Jailani, M.N. Taib, and S. Sulaiman. Color space for psoriasis skin diseases analysis. In *Proc. AsiaSense 2003*, pages 263–268.

[8] I.T. Jolliffe. *Principal Component Analysis*. Springer Series in Statistics, 2002.

[9] L.H. Juang and M.N. Wu. Psoriasis image identification using k-means clustering with morphological processing. *Measurement*, 44(5):895 – 905, 2011.

[10] P. Kakumanu, S. Makrogiannis, and N. Bourbakis. A survey of skin-color modeling and detection methods. *Pattern Recognition*, 40(3):1106–1122, 2007.

[11] M. Kass, A. Witkin, and D. Terzopoulos. Snakes: Active Contour models. *International Journal of Computer Vision*, 1(4):321–331, 1988.

[12] J. Kovac, P. Peer, and F. Solina. Human skin color clustering for face detection. In *Proc. EUROCON 2003*, volume 2, pages 144–148.

[13] S. Kreft, M. Kreft, A. Resman, P. Marko, and K.Z. Kreft. Computer-aided measurement of psoriatic lesion area in a multicenter clinical trial–comparison to physician's estimations. *Journal of Dermatological Science*, 44(1):21–27, 2006.

[14] R.G. Langley and C.N. Ellis. Evaluating psoriasis with psoriasis area and severity index, psoriasis global assessment, and lattice system physician's global assessment. *Journal of the American Academy of Dermatology*, 51(4):563–569, 2004.

[15] B.A. Louden, D.J. Pearce, W. Lang, S.R. Feldman, et al. A Simplified Psoriasis Area Severity Index (SPASI) for rating psoriasis severity in clinic patients. *Dermatology Online Journal*, 10(7), 2004.

[16] J. Röning, R. Jacques, and J. Kontinen. Area assessment of psoriatic lesions based on variable thresholding and subimage classification. In *Proc. Vision Interface 1999*, pages 303–311.

[17] R. Sandhu, T.T. Georgiou, and A.R. Tannenbaum. A new distribution metric for image segmentation. In *Proc. SPIE 2008*, volume 691404, pages 1–9.

[18] R.A. Swerlick and T.J. Lawley. *Harrison's Principles of Internal Medicine*. McGraw-Hill Inc, 2001.

[19] J.S. Taur. Neuro–fuzzy approach to the segmentation of psoriasis images. *Journal of VLSI Signal Processing*, 35(1):19–27, 2003.

[20] J.S. Taur, G.H. Lee, C.W. Tao, C.C. Chen, and C.W. Yang. Segmentation of psoriasis vulgaris images using multiresolution-based orthogonal subspace techniques. *IEEE Transactions on Systems, Man, and Cybernetics, Part B: Cybernetics*, 36(2):390–402, 2006.